
Lookahead Pathology in Monte-Carlo Tree Search

Khôi P. N. Nguyen

Fulbright University Vietnam
Ho Chi Minh City, Vietnam
khoi.nguyen.190037@student.fulbright.edu.vn

Raghuram Ramanujan

Dept. of Mathematics and Computer Science
Davidson College
Davidson, NC 28035 USA
raramanujan@davidson.edu

Abstract

Monte-Carlo Tree Search (MCTS) is an adversarial search paradigm that first found prominence with its success in the domain of computer Go. Early theoretical work established the game-theoretic soundness and convergence bounds for Upper Confidence bounds applied to Trees (UCT), the most popular instantiation of MCTS; however, there remain notable gaps in our understanding of how UCT behaves in practice. In this work, we address one such gap by considering the question of whether UCT can exhibit *lookahead pathology* — a paradoxical phenomenon first observed in Minimax search where greater search effort leads to worse decision-making. We introduce a novel family of synthetic games that offer rich modeling possibilities while remaining amenable to mathematical analysis. Our theoretical and experimental results suggest that UCT is indeed susceptible to pathological behavior in a range of games drawn from this family.

1 Introduction

Monte-Carlo Tree Search (MCTS) is an online planning framework that first found widespread use in game-playing applications [6, 7, 1], culminating in the spectacular success of AlphaGo [30, 31]. MCTS-based approaches have since been successfully adapted to a broad range of other domains, including combinatorial search and optimization [26, 10], malware analysis [27], knowledge extraction [14], and molecule synthesis [12].

Despite these high-profile successes, however, there are still aspects of the algorithm that remain poorly understood. Early theoretical work by Kocsis and Szepesvári introduced the Upper Confidence bounds applied to Trees (UCT) algorithm, now the most widely used variant of MCTS. Their work established that in the limit, UCT correctly identified the optimal action in sequential decision-making tasks, with the regret associated with choosing sub-optimal actions increasing at a logarithmic rate [13]. Coquelin and Munos, however, showed that in the worst-case scenario, UCT’s convergence could take time super-exponential in the depth of the tree [5]. More recent work by Shah *et al.* proposes a “corrected” UCT with better convergence properties [29].

In parallel, there has been a line of experimental work that has attempted to understand the reasons for UCT’s success in practice and characterize the conditions under which it may fail. Ramanujan *et al.* considered the impact of *shallow traps* — highly tactical positions in games like Chess that can be established as wins for the opponent with a relatively short proof tree — and argued that UCT tended to miscalculate such positions [22, 21]. Finnsson and Björnsson considered the performance

of UCT in a set of artificial games and pinpointed *optimistic moves*, a notion similar to shallow traps, as a potential Achilles heel [8]. James *et al.* studied the role of random playouts, a key step in the inner loop of the UCT algorithm, and concluded that the smoothness of the payoffs in the application domain determined the effectiveness of playouts [11]. Our work adds to this body of empirical research, but is concerned with a question that has thus far not been investigated in the literature: *can UCT behave pathologically?*

The phenomenon of *lookahead pathology* was first discovered and analyzed in the 1980s in the context of planning in two-player adversarial domains [3, 17, 20]. Researchers found that in a family of synthetic board-splitting games, deeper Minimax searches counter-intuitively led to worse decision-making. In this paper, we present a novel family of abstract, two-player, perfect information games, inspired by the properties of real games such as Chess, in which UCT-style planning displays lookahead pathology under a wide range of conditions.

2 Background

2.1 Monte-Carlo Tree Search

Consider a planning instance where an agent needs to determine the best action to take in a given state. An MCTS algorithm aims to solve this problem by iterating over the following steps to build a search tree.

- **Selection:** Starting from the root node, we descend the tree by choosing an action at each level according to some policy π . UCT uses UCB1 [2], an algorithm that optimally balances exploration and exploitation in the multi-armed bandit problem, as this selection policy. Specifically, at each state s , UCT selects the action $a = \pi(s)$ that maximizes the following upper confidence bound:

$$\pi(s) = \operatorname{argmax}_a \left(\bar{Q}(T(s, a)) + c \cdot \sqrt{\frac{\log n(s)}{n(T(s, a))}} \right)$$

Here, $T(s, a)$ is the transition function that returns the state that is reached from taking action a in state s , $\bar{Q}(s)$ is the current estimated utility of state s , and $n(s)$ is the visit count of state s . The constant c is a tunable exploration parameter. In adversarial settings, the negamax transformation is applied to the UCB1 formula, to ensure that utilities are alternately maximized and minimized at successive levels of the search tree.

- **Evaluation:** The recursive descent of the search tree using π ends when a node s' that is previously unvisited, or that corresponds to a terminal state (i.e., one from which no further actions are possible), is reached. If s' is non-terminal, then an estimate R of its utility is calculated. This calculation may take the form of random playouts (i.e., the average outcome of pseudorandom completions of the game starting from s'), handcrafted heuristics, or the prediction of a learned estimator like a neural network. For terminal nodes, the true utility of the state is used as R instead. The node s' is then added to the search tree, so that the size of the search tree grows by one after each iteration.
- **Backpropagation:** Finally, the reward R is used to update the visit counts and the utility estimates of each state s that was encountered on the current iteration as follows:

$$\bar{Q}(s) \leftarrow \frac{n(s)\bar{Q}(s) + R(s)}{n(s) + 1} \quad n(s) \leftarrow n(s) + 1$$

This update assigns to each state the average reward accumulated from every episode that passed through it.

We repeat the above steps until the designated computational budget is met; at that point, the agent selects the action $a = \operatorname{argmax}_{a'} Q(T(r, a'))$ to execute at the root node r .

2.2 Lookahead Pathology

Searching deeper is generally believed to be more beneficial in planning domains. Indeed, advances in hardware that permitted machines to tractably build deeper Minimax search trees for Chess were a

key reason behind the success of Deep Blue [4]. However, there are settings in which this property is violated, such as the P-games investigated by several researchers in the 1980s [3, 17, 20]. Over the years, many have attempted to explain the causes of pathology and why it is not encountered in real games like Chess. Nau *et al.* reconciled these different proposals and offered a unified explanation that focused on three factors: the branching factor of the game, the degree to which the game demonstrates *local similarity* (a measure of the correlation in the utilities of nearby states in the game tree), and the *granularity* of the heuristic function used (the number of distinct values that the heuristic takes on) [16]. They concluded that pathology was most pronounced in games with a high branching factor, low local similarity and low heuristic granularity.

2.3 Synthetic Game Tree Models

There is a long tradition of using abstract, artificial games to empirically understand the behavior of search algorithms. The P-game model is a notable example, that constructs a game tree in a bottom-up fashion [19]. To create a P-game instance, the values of the leaves of the tree are carefully set to win/loss values [19], though variants using real numbers instead have also been studied [15]. The properties of the tree arise organically from the distribution used to set the leaf node values. P-games were the subject of much interest in the 1980s, as the phenomenon of lookahead pathology was first discovered in the course of analyzing the behavior of Minimax search in this setting [3, 17]. While the model’s relative simplicity allows for rigorous mathematical analysis, P-games also suffer from a couple of drawbacks. Firstly, computing the value of the game and the minimax value of the internal nodes requires search, and that all the leaf nodes of the tree be retained in memory, which restricts the size of the games that may be studied in practice. Secondly, the construction procedure only models a narrow class of games, namely, ones where the values of leaf nodes are independent of each other.

Other researchers have proposed top-down models, where each internal node of the tree maintains some state information that is incrementally updated and passed down the tree. The value of a leaf node is then determined by a function of the path that was taken to reach it. For example, in the models studied by Nau and Scheucher and Kaindl, values are assigned to the edges in the game tree and the utility of a leaf node is determined by the sum of the edge values on the path from the root node to the leaf [18, 28]. These models were used to demonstrate that correlations among sibling nodes were sufficient to eliminate lookahead pathology in Minimax. However, search is still required to determine the true value of internal nodes, thereby only allowing for the study of small games. Furtak and Buro proposed *prefix value trees* that extend the model of Scheucher and Kaindl by observing that the minimax value of nodes along a principal variation can never worsen for the player on move [9]. Setting the values of nodes while obeying this constraint during top-down tree construction obviates the need for search, which allowed them to generate arbitrarily large games.

Finally, synthetic game tree models have also been used to study the behavior of MCTS algorithms like UCT. For example, Finnsson and Björnsson used variations of Chess to identify the features of the search space that informed the success and failure of UCT [8]. Ramanujan *et al.* studied P-games augmented with “critical moves” — specific actions that an agent must get right at important junctures in the game to ensure victory [23]. We refine this latter idea and incorporate it into a top-down model, which we present in the following section.

3 Critical Win-Loss Games

Our goal in this paper is to determine the conditions under which UCT exhibits lookahead pathology. To conduct this study, we seek a class of games that satisfy several properties. Firstly, we desire a model that permits us to construct arbitrarily large games to more thoroughly study the impact of tree depth on UCT’s performance. We note that most of the game tree models discussed in Section 2.3 do not meet this requirement. The one exception is the prefix value tree model of Furtak and Buro that, however, fails a different test: the ability to construct games with parameterizable difficulty. Specifically, we find that prefix value games are too “easy” as evidenced by the fact that a naïve planning algorithm that combines minimal lookahead with purely random playouts achieves perfect decision-making accuracy in this setting (see Appendix A for a proof of this claim). In this section, we describe *critical win-loss games*, a new generative model of extensive-form games, that addresses both these shortcomings of existing models.

3.1 Game Tree Model

Our model generates game trees in a top-down fashion, assigning each node a true utility of either $+1$ or -1 . In principle, every state in real games like Chess or Go can be labeled in a similar fashion (ignoring the possibility of draws) with their true game-theoretic values. Thus, we do not lose any modeling capacity by limiting ourselves to just win-loss values. The true minimax value of a state imposes constraints on the values of its children as noted by Furtak and Buro — in our setting, this leads to two kinds of internal tree nodes. A *forced node* is one with value -1 ($+1$) at a maximizing (minimizing) level. All the children of such a node are constrained to also be -1 ($+1$). A *choice node*, on the other hand, is one with value $+1$ (-1) at a maximizing (minimizing) level. At least one child of such a node must have the same minimax value as its parent. Figure 1 presents examples of these concepts.

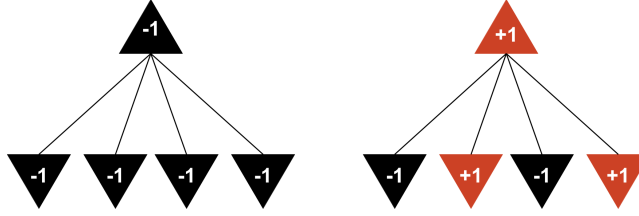


Figure 1: An example of a forced node (left) and a choice node (right). Upward-facing triangles represent maximizing nodes while downward-facing triangles represent minimizing nodes.

All the variation that is observed in the structures of different game trees is completely determined by what happens at choice nodes. As noted earlier, *exactly* one child of a choice node must share the minimax value of its parent; the values of the remaining children are unconstrained. We introduce a parameter called the *critical rate* (γ) that determines the values of these unconstrained children. We now describe our procedure for growing a critical win-loss tree rooted at a node s with minimax value $v(s)$:

- Let $S = \{s_1, s_2, \dots, s_b\}$ denote the b children of s .
- If s is a forced node, then we set $v(s_1) = v(s_2) = \dots = v(s_b) = v(s)$, and continue recursively growing each subtree.
- If s is a choice node, then we pick an $s_i \in \{s_1, \dots, s_b\}$ uniformly at random and set $v(s_i) = v(s)$, designating s_i to be the child that corresponds to the optimal action choice at s . For all s_j such that $j \neq i$, we set $v(s_j) = -v(s)$ with probability γ and we set $v(s_j) = v(s)$ with probability $1 - \gamma$, before recursively continuing to grow each subtree.

We make several observations about the trees grown by this model. Firstly, one can apply the above growth procedure in a lazy manner, so that only those parts of the game tree that are actually reached by the search algorithm need to be explicitly generated. Thus, the size of the games is only limited by the amount of search effort we wish to expend. Secondly, the critical rate parameter serves as a proxy for game difficulty. At one extreme, if $\gamma = 0$, then every child at every choice node has the same value as its parent — in effect, there are no “wrong” moves for either player, and planning becomes trivial. At the other extreme, if $\gamma = 1$, then every sub-optimal move at every choice node leads to a loss and the game becomes unforgiving. A single blunder at any stage of the game instantly hands the initiative to the opponent. Figure 2 gives examples of game trees generated with different settings of γ . For the sake of simplicity, we focus on trees with a uniform branching factor b in this study.

3.2 Critical Rates in Real Games

Before proceeding, we pause to validate our model by measuring the critical rates of positions in Chess (see Appendix E for similar data on Othello). We begin by first sampling a large set of positions that are p plies deep into the game. These samples are gathered using two different methods:

- *Light playouts*: each side selects among the legal moves uniformly at random.

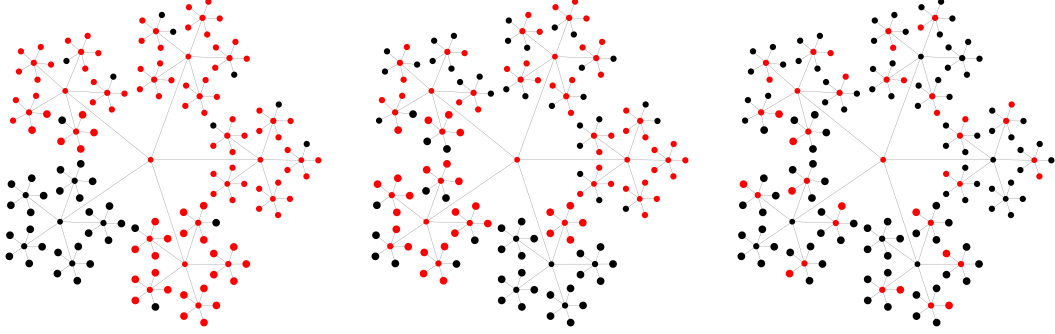


Figure 2: Effect of critical rate (γ) on game tree structure. Nodes in red correspond to $+1$ nodes, while nodes in black correspond to -1 nodes, with the root node in the center. The tree instances were generated with $\gamma = 0.1$, $\gamma = 0.5$, and $\gamma = 1.0$, from left to right.

- *Heavy playouts*: each side runs a 10-ply search using the Stockfish 13 Chess engine [25] (freely available online under a GNU GPL v3.0 license) and then selects among the top-3 moves uniformly at random.

We approximate $v(s)$ for these sampled states using deep Minimax searches. Specifically, we use $v(s) \approx \text{sgn}(\tilde{v}_d(s))$, where $\tilde{v}_d(s)$ denotes the result of a d -ply Stockfish search. To compute the empirical critical rate $\tilde{\gamma}(s)$ for a particular choice node s , we begin by computing $\tilde{v}_{20}(s)$ and $\tilde{v}_{19}(s')$ for all the children s' of s and then calculate:

$$\tilde{\gamma}(s) = \frac{1}{b-1} \sum_{s'} \mathbb{1}[\text{sgn}(\tilde{v}_{19}(s')) \neq \text{sgn}(\tilde{v}_{20}(s))]$$

Admittedly, using the outcome of a deep search as a stand-in for the true game theoretic value of a state is not ideal. However, strong Chess engines are routinely used in this manner as analysis tools by humans, and we thus believe this to be a reasonable approach. Figure 3 presents histograms of $\tilde{\gamma}$ data collected for $p = 10$ and $p = 36$, using both light and heavy playouts. Each histogram aggregates data over $\sim 20,000$ positions.

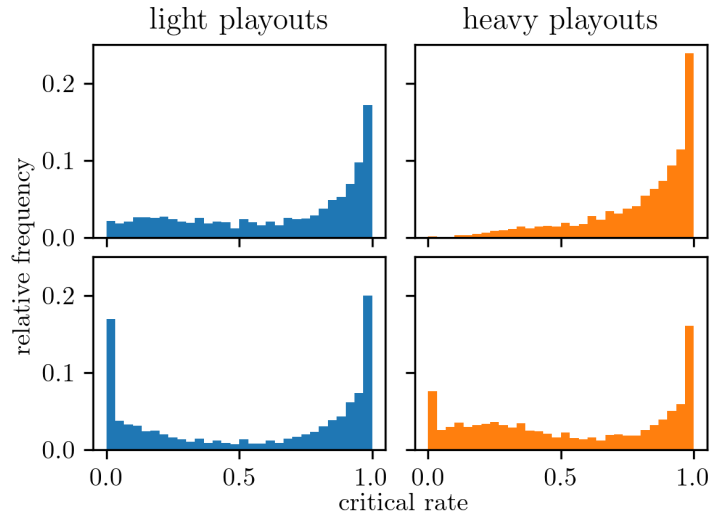


Figure 3: Histograms of empirical critical rates ($\tilde{\gamma}$) for Chess positions sampled $p = 10$ (top row) and $p = 36$ (bottom row) plies deep into the game. We sample the positions using both light playouts (left column) and heavy playouts (right column).

We note that about 40–50% of the positions sampled have $\tilde{\gamma}$ values higher than 0.9, which is consistent with Chess’s reputation for being a highly tactical game. We also see that the $\tilde{\gamma}$ values collected

for Chess form a distribution that is non-stationary with respect to game progression, unlike in our proposed game tree model where γ is fixed to be a constant. Nonetheless, we believe that this simplification in our modeling is reasonable: at deeper plies, the distribution of $\tilde{\gamma}$ becomes strikingly bimodal, with most of the mass accumulating in the ranges $[0.0, 0.1]$ and $[0.9, 1.0]$. This clustering means that one could partition Chess game tree into two very different kinds of subgames (with high and low γ), within each of which the critical rate remains within a narrow range.

3.3 Heuristic Design

Before we can run UCT search experiments on critical win-loss games, we need to resolve one more issue: *how should UCT estimate the utility of non-terminal nodes?* One popular approach to constructing artificial heuristics is the additive noise model — the heuristic estimate $h(s)$ for a node s is computed as $h(s) = v(s) + \epsilon$, where ϵ is a random variable drawn from a standard distribution, like a Gaussian [15, 24]. However, as we will see, static evaluations of positions in real games often follow complex distributions.

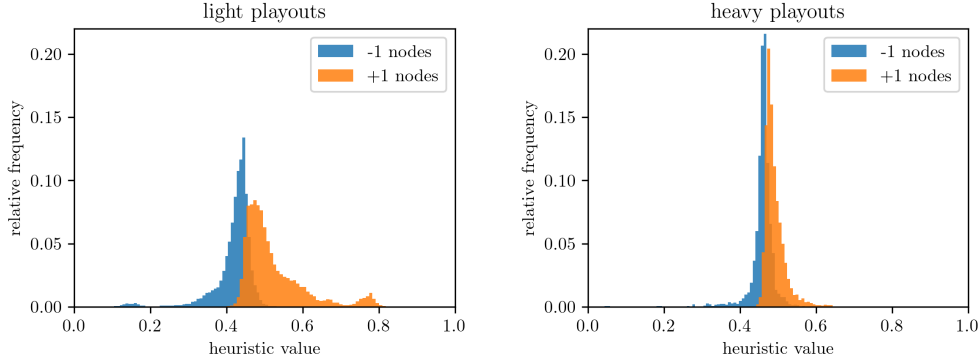


Figure 4: Distribution of Stockfish 13 static evaluations of $+1$ and -1 positions sampled $p = 10$ plies deep into Chess. The positions are sampled using both light playouts (left) and heavy playouts (right).

To better understand the behavior of heuristic functions in real games, we once again turn to Chess and the Stockfish engine. We sample $\sim 100,000$ positions each using light and heavy playouts for $p = 10$. As before, we use $\text{sgn}(\tilde{v}_{20}(s))$ as a proxy for $v(s)$ for each sampled state s . We also compute $\tilde{v}_0(s)$ for each s , which we normalize to the range $[0, 1]$ — this is the static evaluation of each s without any lookahead. Figure 4 presents histograms of $\tilde{v}_0(s)$, broken out by $v(s)$. A clearer separation between the orange and blue histograms (i.e., between the evaluations of $+1$ and -1 nodes) indicates that the heuristic is better at telling apart winning positions from losing ones. Indeed, the ideal heuristic would score every $+1$ position higher than every -1 position, thus ordering them perfectly. We see in Figure 4 that such clear sorting does not arise in practice in Chess, particularly for positions that are encountered with strong play. Moreover, the valuations assigned to positions do not follow a Gaussian distribution, and attempts to model them as such are likely too simplistic. However, these histograms also suggest an empirical method for generating heuristic valuations of nodes — we can treat the histograms as probability density functions and sample from them. For example, to generate a heuristic estimate for a -1 node s in our synthetic game, we can draw $h(s) \in [0, 1]$ according to the distribution described by one of the blue histograms in Figure 4. Of course, given the sensitivity of the shape of these histograms to the sampling parameters, it is natural to wonder *which* histogram should be used. Rather than make an arbitrary choice, we run experiments using a diverse set of such histogram-based heuristics, generated from different choices of p , different playout sampling strategies, and different game domains.

Additionally, we note that one can also use random playouts as heuristic evaluations, like in the original formulation of UCT. One advantage of our critical win-loss game tree model is that we can analytically characterize the density of $+1$ and -1 nodes at a depth d from the root node, given a critical rate γ and branching factor b . Specifically, for a tree rooted at a maximizing choice node, the

density of +1 nodes at depths $2d$ and $2d + 1$ (denoted as f_{2d} and f_{2d+1} respectively) are given by:

$$f_{2d} = k^{2d} + \frac{1 - k^{2d+2}}{1 + k} \quad (1)$$

$$f_{2d+1} = f_{2d} \cdot k \quad (2)$$

where $k = 1 - \gamma + \gamma/b$. We refer the reader to Appendix B for the relevant derivations. Access to these expressions means that we can cheaply simulate random playouts of depth $2d$: the outcome of a single playout (ℓ_1) corresponds to sampling from the set $\{+1, -1\}$ with probabilities f_{2d} and $1 - f_{2d}$ respectively. For lower variance estimates, we can use the mean of this distribution instead, which would correspond to averaging the outcomes of a large number of playouts (ℓ_∞). In our experiments, we explore the efficacy of the heuristics ℓ_1 and ℓ_∞ as well.

4 Results

4.1 Theoretical Analysis

We begin with our main theoretical result and provide a sketch of the proof.

Theorem 1. *In a critical win-loss game with $\gamma = 1.0$, UCT with a search budget of N nodes will exhibit lookahead pathology for choices of the exploration parameter $c \geq \sqrt{\frac{N^3}{2 \log N}}$, even with access to a perfect heuristic.*

The key observation underpinning the result is that the densities of +1 nodes in both the optimal and sub-optimal subtrees rooted at a choice node (given by equations (1) and (2)) begin to approach the same value for large enough depths. This in turn suggests a way to lead UCT astray, namely to force UCT to over-explore so that it builds a search tree in a breadth-first manner. In such a scenario, the converging +1 node densities in the different subtrees, together with the averaging back-up mechanism in the algorithm, leaves UCT unable to tell apart the utilities of its different action choices. Notably, this happens even though we provide perfect node evaluations to UCT (i.e., the true minimax value of each node) — the error arises purely due to the structural properties of the underlying game tree. All that remains to be done is to characterize the conditions under which this behavior can be induced, which is presented in detail in Appendix C. Our experimental results suggest that the bound in Theorem 1 can likely be tightened, since in practice, we often encounter pathology at much lower values for c than expected. We further find that the pathology persists even when we relax the assumption that $\gamma = 1.0$, as described in the following sections.

4.2 Experimental Setup

We now describe our experimental methodology for investigating pathology in UCT. Without loss of generality, we focus on games that are rooted at maximizing choice nodes (i.e., root node has a value of +1). We set the maximum game tree depth at 50, which ensures that relatively few terminal nodes are encountered within the search horizon (other depths are explored in the supplementary material, see Appendix F). We present results from a 4-factor experimental design: 2 choices of critical rate (γ) \times 3 choices of branching factor (b) \times 2 choices of heuristic models \times 5 choices of the UCT exploration constant (c). A larger set of results, exploring a wider range of these parameter settings, is presented in Appendices F–H. For each chosen parameterization, we generate 500 synthetic games using our critical win-loss tree model. We run UCT with different computational budgets on each of these trees, as measured by the number of search iterations (i.e., the size of the UCT search tree). We define the *decision accuracy* (denoted as δ_i) to be the number of times that UCT chose the correct action at the root node, when run for i iterations, averaged across the 500 members of each tree family sharing the same parameter settings. Our primary performance metric is the *pathology index* \mathcal{P}_j defined as:

$$\mathcal{P}_j = \frac{\delta_j}{\delta_{10}}$$

where $j \in \{10, 10^2, 10^3, 10^4, 10^5\}$. Values of $\mathcal{P}_j < 1$ indicate that additional search effort leads to worse outcomes (i.e., pathological behavior), while $\mathcal{P}_j > 1$ indicates that search is generally beneficial. We ran our experiments on an internal cluster of Intel Xeon Gold 5128 3.0GHz CPUs with 512G of

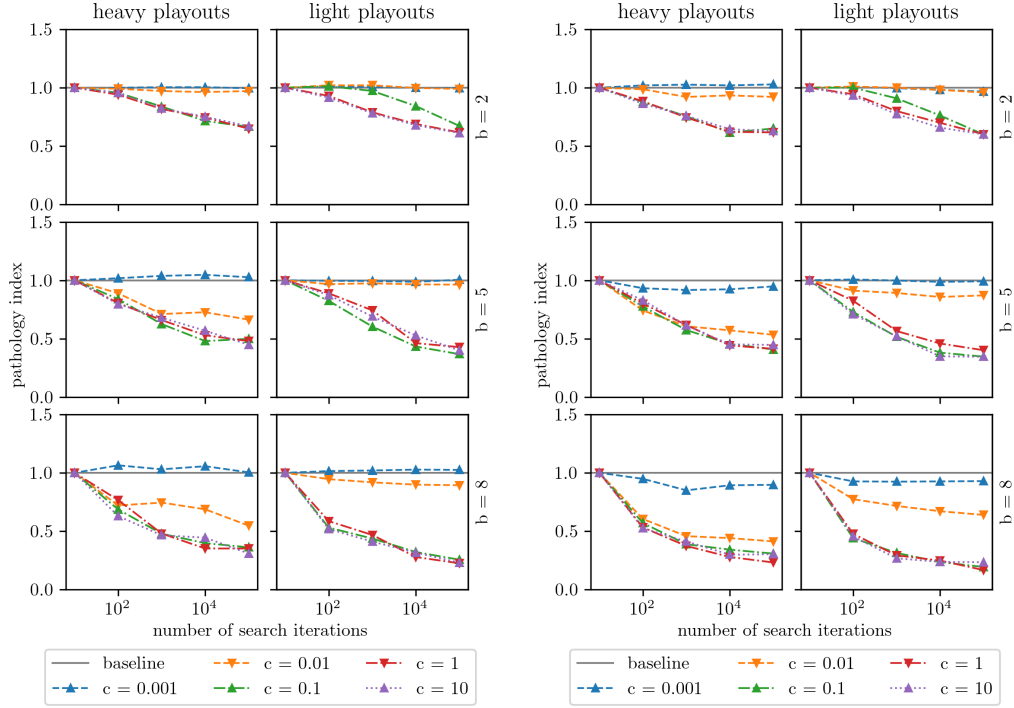


Figure 5: Measuring pathological behavior in UCT on critical win-loss games of depth 50 with $\gamma = 0.9$ (left) and $\gamma = 1$ (right). The heuristic to guide UCT is constructed from histograms of Stockfish evaluations of positions sampled at depth 10, using both light and heavy playouts. Each colored line corresponds to an instantiation of UCT with a different exploration constant. Note that the x -axis is plotted on a log-scale.

RAM. We estimate that replicating the full set of results presented in this paper, with 96 jobs running in parallel, would take about three weeks of compute time on a similar system. The code for reproducing our experiments is hosted at <https://github.com/redacted-for-double-blind-review>.

4.3 Discussion

Figure 5 presents our main results. Our chief finding is that the choice of γ is the biggest determinant of pathological behavior in UCT. For games generated with $\gamma = 1$, we find that UCT exhibits lookahead pathology *regardless* of all other parameters — the exploration constant, the branching factor, or how the heuristic is constructed. Appendices F and H confirm the robustness of this result using additional data collected for other game tree depths and for heuristics constructed using data collected from Othello. For smaller values of γ , the effect is not as strong and other factors begin to play a role. For example, with $\gamma = 0.9$, pathological behavior is most apparent at higher branching factors and with more uniform exploration strategies (i.e., higher settings of c), consistent with Theorem 1. For $\gamma = 0.5$, pathology is almost completely absent, regardless of other parameters (see Appendix G).

We also find that random playouts provide limited signal for guiding planning algorithms in this domain, even in modestly deep trees. This is because equations (1) and (2) (and their duals for -1 nodes) which describe the density of $+1/-1$ nodes quickly approach their limiting distribution. In practice, this means that $+1$ and -1 nodes that are more than ~ 20 plies removed from the end of the game receive identical evaluations, resulting in random decision-making at the root node in most cases.

Finally, for the sake of completeness, we also evaluate the performance of Minimax search with alpha-beta pruning on our critical win-loss games. These results are presented in Appendix I. We find

that Minimax is even more susceptible to lookahead pathology than UCT in our setting, exhibiting pathology at γ values as low as 0.5. Indeed, our results indicate that lookahead pathology in Minimax search can arise even in games with low branching factor ($b = 2$), modest local similarity ($\gamma = 0.5$) and with a highly granular heuristic (in this case, derived from binning Stockfish’s evaluation function and treating that as a distribution), which runs counter to the findings of Nau *et al.* [16]. While reconciling these results is an important next step, we defer that investigation to future work as it is beyond the scope of this paper.

4.4 Broader Impacts

This paper highlights a counter-intuitive failure mode for MCTS that deserves broader appreciation and recognition from researchers and practitioners. The fact that UCT has the potential to make worse decisions when given additional compute time means that the algorithm needs to be used with greater care. We recommend that users generate scaling plots such as those shown in Figure 5 to better understand whether UCT is well-behaved in their particular application domain, before wider deployment.

5 Conclusions

In this paper, we explored the question of whether MCTS algorithms like UCT could exhibit lookahead pathology — an issue hitherto overlooked in the literature. Due to the shortcomings of existing synthetic game tree models, we introduced our own novel generative model for extensive-form games. We used these critical win-loss games as a vehicle for exploring search pathology in UCT and found it to be particularly pronounced in high critical rate regimes. Important avenues for follow-up work include generalizing the theoretical results presented in this paper to games where $\gamma \neq 1$ and deriving tighter bounds for the exploration parameter c , as well as investigating whether such pathologies emerge in real-world domains.

References

- [1] Broderick Arneson, Ryan B. Hayward, and Philip Henderson. Monte carlo tree search in hex. *IEEE Transactions on Computational Intelligence and AI in Games*, 2(4):251–258, 2010.
- [2] Peter Auer, Nicolò Cesa-Bianchi, and Paul Fischer. Finite-time analysis of the multiarmed bandit problem. *Machine Learning*, 47(2):235–256, May 2002.
- [3] Donald F. Beal. An analysis of minimax. *Advances in Computer Chess 2*, pages 103–109, 1980.
- [4] Murray Campbell, A. Joseph Hoane, and Feng hsiung Hsu. Deep blue. *Artificial Intelligence*, 134(1):57–83, 2002.
- [5] Pierre-Arnaud Coquelin and Rémi Munos. Bandit algorithms for tree search. In *Proceedings of the Twenty-Third Conference on Uncertainty in Artificial Intelligence*, UAI’07, page 67–74, Arlington, Virginia, USA, 2007. AUAI Press.
- [6] Rémi Coulom. Efficient selectivity and backup operators in monte-carlo tree search. In *Computers and Games*, pages 72–83, Berlin, Heidelberg, 2007. Springer Berlin Heidelberg.
- [7] Hilmar Finnsson and Yngvi Björnsson. Simulation-based approach to general game playing. In *AAAI ’08*, page 259–264. AAAI Press, 2008.
- [8] Hilmar Finnsson and Yngvi Björnsson. Game-tree properties and MCTS performance. In *IJCAI 2011 Workshop on General Intelligence in Game Playing Agents*, pages 23–30, 2011.
- [9] Timothy Furtak and Michael Buro. Minimum proof graphs and fastest-cut-first search heuristics. In *IJCAI ’09*, page 492–498, San Francisco, CA, USA, 2009. Morgan Kaufmann Publishers Inc.
- [10] Jack Goffinet and Raghuram Ramanujan. Monte-carlo tree search for the maximum satisfiability problem. In *Principles and Practice of Constraint Programming*, pages 251–267, Cham, 2016. Springer International Publishing.
- [11] Steven James, George Konidaris, and Benjamin Rosman. An analysis of monte carlo tree search. *Proceedings of the AAAI Conference on Artificial Intelligence*, 31(1), Feb. 2017.

- [12] Seiji Kajita, Tomoyuki Kinjo, and Tomoki Nishi. Autonomous molecular design by monte-carlo tree search and rapid evaluations using molecular dynamics simulations. *Communications Physics*, 3(1):77, May 2020.
- [13] Levente Kocsis and Csaba Szepesvári. Bandit based monte-carlo planning. In *Proceedings of the 17th European Conference on Machine Learning, ECML’06*, page 282–293, Berlin, Heidelberg, 2006. Springer-Verlag.
- [14] Guiliang Liu, Xu Li, Jiakang Wang, Mingming Sun, and Ping Li. *Extracting Knowledge from Web Text with Monte Carlo Tree Search*, page 2585–2591. Association for Computing Machinery, New York, NY, USA, 2020.
- [15] Mitja Luštrek, Matjaž Gams, and Ivan Bratko. Why minimax works: an alternative explanation. In *IJCAI ’05*, pages 212–217, Edinburgh, Scotland, 2005.
- [16] Dana S. Nau, Mitja Luštrek, Austin Parker, Ivan Bratko, and Matjaž Gams. When is it better not to look ahead? *Artificial Intelligence*, 174(16):1323–1338, 2010.
- [17] Dana S. Nau. An investigation of the causes of pathology in games. *Artificial Intelligence*, 19(3):257–278, 1982.
- [18] Dana S. Nau. Pathology on game trees revisited, and an alternative to minimaxing. *Artificial Intelligence*, 21(1-2):221–244, 1983.
- [19] Judea Pearl. Asymptotic properties of minimax trees and game-searching procedures. *Artificial Intelligence*, 14(2):113–138, 1980.
- [20] Judea Pearl. On the nature of pathology in game searching. *Artificial Intelligence*, 20(4):427–453, 1983.
- [21] Raghuram Ramanujan and Bart Selman. Trade-offs in sampling-based adversarial planning. In *ICAPS 2011, Freiburg, Germany June 11-16, 2011*. AAAI, 2011.
- [22] Raghuram Ramanujan, Ashish Sabharwal, and Bart Selman. On adversarial search spaces and sampling-based planning. In *ICAPS 2010, Toronto, Ontario, Canada, May 12-16, 2010*, pages 242–245. AAAI, 2010.
- [23] Raghuram Ramanujan, Ashish Sabharwal, and Bart Selman. Understanding sampling style adversarial search methods. In *UAI 2010, Catalina Island, CA, USA, July 8-11, 2010*, pages 474–483. AUAI Press, 2010.
- [24] Raghuram Ramanujan, Ashish Sabharwal, and Bart Selman. On the behavior of UCT in synthetic search spaces. In *ICAPS 2011 Workshop on Monte Carlo Tree Search: Theory and Applications, Freiburg, Germany June 12, 2011*, 2011.
- [25] Tord Romstad, Marco Costalba, Joona Kiiski, and G Linscott. Stockfish: A strong open source chess engine. *Open Source available at <https://stockfishchess.org/>*. Retrieved November 29th, 2017.
- [26] Ashish Sabharwal, Horst Samulowitz, and Chandra Reddy. Guiding combinatorial optimization with uct. In *CPAIOR 2012*, page 356–361, Berlin, Heidelberg, 2012. Springer-Verlag.
- [27] Riccardo Sarteau and Alessandro Farinelli. A monte carlo tree search approach to active malware analysis. In *IJCAI-17*, pages 3831–3837, 2017.
- [28] Anton Scheucher and Hermann Kaindl. Benefits of using multivalued functions for minimaxing. *Artificial Intelligence*, 99(2):187 – 208, 1998.
- [29] Devavrat Shah, Qiaomin Xie, and Zhi Xu. Non-asymptotic analysis of monte carlo tree search. In *Abstracts of the 2020 SIGMETRICS/Performance Joint International Conference on Measurement and Modeling of Computer Systems, SIGMETRICS ’20*, page 31–32, New York, NY, USA, 2020. Association for Computing Machinery.
- [30] David Silver, Aja Huang, Chris J. Maddison, Arthur Guez, Laurent Sifre, George van den Driessche, Julian Schrittwieser, Ioannis Antonoglou, Veda Panneershelvam, Marc Lanctot, Sander Dieleman, Dominik Grewe, John Nham, Nal Kalchbrenner, Ilya Sutskever, Timothy Lillicrap, Madeleine Leach, Koray Kavukcuoglu, Thore Graepel, and Demis Hassabis. Mastering the game of go with deep neural networks and tree search. *Nature*, 529(7587):484–489, Jan 2016.
- [31] David Silver, Julian Schrittwieser, Karen Simonyan, Ioannis Antonoglou, Aja Huang, Arthur Guez, Thomas Hubert, Lucas Baker, Matthew Lai, Adrian Bolton, Yutian Chen, Timothy Lillicrap, Fan Hui, Laurent Sifre, George van den Driessche, Thore Graepel, and Demis Hassabis. Mastering the game of go without human knowledge. *Nature*, 550(7676):354–359, Oct 2017.

Supplementary Material

A On Planning in Prefix Value Trees

In a prefix value (PV) tree, the values of nodes are drawn from the set of integers, with positive values representing wins for the maximizing player (henceforth, Max) and the rest indicating wins for the minimizing player (Min). For the sake of simplicity, we disallow draws. Let $m(v)$ represent the minimax value of a node v . We grow the subtree rooted at v as follows:

- Let $V = \{v_1, v_2, \dots, v_b\}$ represent the set of children of v , corresponding to action choices $A = \{a_1, a_2, \dots, a_b\}$.
- Pick an $a_i \in A$ uniformly at random — this is designated to be the optimal action choice at v .
- Assign $m(v_i) = m(v)$. If Max is on move at v , then $m(v_j) = m(v) - k, \forall j \neq i$. If Min is on move v , then $m(v_j) = m(v) + k, \forall j \neq i$.

Here, k is a constant that represents the cost incurred by the player on move for taking a sub-optimal action. The depth of the tree is controlled by the parameter d_{max} and a uniform branching factor of b is assumed.

The PV tree model, is an attractive object of study as despite its relative simplicity, it captures a very rich class of games. However, it has one major drawback: a simple 1-ply lookahead search, using the average outcome of random playout trajectories as a heuristic, achieves very high decision accuracies. We now explore this phenomenon a little deeper.

Without loss of generality, we restrict our attention to trees where Max is on move at the root node n . Moreover, we require that $m(n) = 1$ and that n has exactly one optimal child — this ensures that our search algorithm is faced with a non-trivial decision at the root node. While we focus on the case where $b = 2$ in what follows, extending our results to higher branching factors is straightforward. We denote the left and right children of n by l and r respectively and assume that l is the optimal move. Define $S_d(v)$ to be the sum of the minimax values of the leaf nodes in the subtree of depth d rooted at node v .

Proposition 1. $S_d(l) - S_d(r) = 2^d$ for all $d \geq 0$.

Proof. We proceed by induction on d . For the base case, $S_0(l) - S_0(r) = 1 - 0 = 2^0$ by definition. Assume the claim holds for $d = t, t \geq 0$, where t is a Max level. Then, $S_{t+1}(l) - S_{t+1}(r) = (S_t(l) + (S_t(l) - k)) - (S_t(r) + (S_t(r) - k)) = 2(S_t(l) - S_t(r)) = 2 \cdot 2^t = 2^{t+1}$. A symmetric argument can be made for the case where t is a Min level. \square

Define $P(v)$ to be the average outcome of random playouts performed from the node v . If the subtree rooted at v has uniform depth d , then $\mathbb{E}[P(v)] = S_d(v)/2^d$. An immediate consequence of Proposition 1 is that $\mathbb{E}[P(l)] - \mathbb{E}[P(r)] = (S_d(l) - S_d(r))/2^d = 1$, for any depth d , i.e., in the limit, the estimated utility of the optimal move l at the root will always be greater than that of r . In other words, the decision accuracy of a 1-ply lookahead search informed by random playouts approaches 100% with increasing number of playouts, independent of the depth of the tree. It is straightforward to extend this result to the case even when k is a random variable, drawn uniformly at random from some set $\{1, \dots, k_{max}\}$.

B On the Distribution of Leaf Node Values in Critical Win-Loss Games

In this section, we analyze the density of $+1$ nodes in critical win-loss game as a function of its depth (d), branching factor (b) and critical rate (γ). We limit ourselves to the case where b is uniform, $b \geq 2$ and $0 < \gamma \leq 1$.

Without loss of generality, we assume that the root is a maximizing choice node (i.e., has a minimax value of +1). Then, the expected number of its +1 children is:

$$1 + (1 - \gamma) \cdot (b - 1) = b + \gamma - b\gamma$$

We denote the expected *density* of these +1 children (among the possible b children) by k , where:

$$k = \frac{b + \gamma - b\gamma}{b} = 1 - \gamma + \frac{\gamma}{b} \quad (3)$$

We note that by a symmetric argument, this expression also captures the density of the -1 children of a minimizing choice node.

Now consider a critical win-loss game instance rooted at a maximizing choice node. Let f_n denote the +1 density at depth n in this tree. We will calculate a closed-form expression for f_n . When n is even (i.e., Max is on move), we have the following recursive relationship due to equation (3):

$$f_{n+1} = f_n \cdot \left(1 - \gamma + \frac{\gamma}{b}\right)$$

Substituting $2d$ for n , we have:

$$f_{2d+1} = f_{2d} \cdot k \quad (4)$$

When n is odd (i.e., Min is on move), the choice nodes have value -1 . Once again using equation (3), we derive the following recursive equation for -1 nodes:

$$\begin{aligned} 1 - f_{n+1} &= (1 - f_n) \cdot \left(1 - \gamma + \frac{\gamma}{b}\right) \\ f_{n+1} &= 1 - (1 - f_n) \left(1 - \gamma + \frac{\gamma}{b}\right) \\ f_{n+1} &= f_n \cdot k + 1 - k \end{aligned}$$

Substituting $2d + 1$ for n , we have:

$$f_{2d+2} = f_{2d+1} \cdot k + 1 - k \quad (5)$$

From equations (4) and (5), we have:

$$f_{2d+2} = f_{2d} \cdot k^2 + (1 - k)$$

By induction, we can then derive the following non-recurrent formula for f_{2d} :

$$f_{2d} = f_0 \cdot (k^2)^d + (1 - k) \cdot \frac{1 - (k^2)^{d+1}}{1 - k^2}$$

where $f_0 = 1$. Simplifying, we have:

$$f_{2d} = k^{2d} + \frac{1 - k^{2d+2}}{1 - k^2}$$

If we now allow $d \rightarrow \infty$, we have:

$$\lim_{d \rightarrow \infty} f_{2d} = \frac{1 - k}{1 - k^2} = \frac{1}{1 + k} = \frac{1}{2 - \gamma + \frac{\gamma}{b}} \quad (6)$$

and:

$$\lim_{d \rightarrow \infty} f_{2d+1} = \lim_{d \rightarrow \infty} f_{2d} \cdot k = \frac{k}{1 + k} = \frac{1 - \gamma + \frac{\gamma}{b}}{2 - \gamma + \frac{\gamma}{b}} \quad (7)$$

C Pathology Bound for UCT

We provide a proof of Theorem 1 from Section 4.1, which is restated below.

Theorem 1. *In a critical win-loss game with $\gamma = 1.0$, UCT with a search budget of N nodes will exhibit lookahead pathology for choices of the exploration parameter $c \geq \sqrt{\frac{N^3}{2 \log N}}$, even with access to a perfect heuristic.*

Proof. The proof consists of two parts. First, we argue that with an appropriately chosen value for the exploration constant c , UCT will build a balanced search tree in a breadth-first fashion. Then, we show that such a tree building strategy will cause UCT's decision accuracy to devolve to random guessing with increased search effort. Consider a node p with b children. Let a_1 and a_2 denote two of these children such that $n(a_1) < n(a_2)$. Our aim is to find a value for the exploration parameter c such that the UCB1 formula will prioritize visiting a_1 over a_2 , regardless of the difference in their (bounded) utility estimates. This amounts to UCT building a search tree in a breadth-first fashion.

Without loss of generality, assume p is a maximizing node. For UCT to visit a_1 before a_2 on the next iteration, we must have:

$$\bar{Q}(a_1) + c\sqrt{\frac{\log n(p)}{n(a_1)}} > \bar{Q}(a_2) + c\sqrt{\frac{\log n(p)}{n(a_2)}}$$

Rearranging terms, this is equivalent to the condition:

$$c > \frac{\bar{Q}(a_2) - \bar{Q}(a_1)}{\sqrt{\log n(p)} \left(\sqrt{\frac{1}{n(a_1)}} - \sqrt{\frac{1}{n(a_2)}} \right)} \quad (8)$$

We will now bound the right-hand side of equation 8 in terms of our search budget N . Firstly, since the heuristic estimates of nodes are bounded by $[0, 1]$, we know that $\bar{Q}(a) \in [0, 1]$ for any node a . We can therefore bound the numerator of equation (8) from above as:

$$\bar{Q}(a_2) - \bar{Q}(a_1) \leq 1 \quad (9)$$

Now we turn our attention to the denominator D of equation (8). We have:

$$\begin{aligned} D &= \sqrt{\log n(p)} \left(\sqrt{\frac{1}{n(a_1)}} - \sqrt{\frac{1}{n(a_2)}} \right) \\ &= \sqrt{\log n(p)} \left[\frac{n(a_2) - n(a_1)}{\sqrt{n(a_1)n(a_2)}(\sqrt{n(a_1)} + \sqrt{n(a_2)})} \right] \\ &\geq \sqrt{\log n(p)} \left[\frac{1}{\sqrt{n(a_1)n(a_2)}(\sqrt{n(a_1)} + \sqrt{n(a_2)})} \right] && \text{since } n(a_2) > n(a_1) \\ &\geq \sqrt{\log n(p)} \left[\frac{1}{\frac{n(a_1)+n(a_2)}{2}(\sqrt{n(a_1)} + \sqrt{n(a_2)})} \right] && \text{by the AM-GM inequality} \\ &\geq \sqrt{\log n(p)} \left[\frac{1}{\frac{n(a_1)+n(a_2)}{2} \sqrt{2(n(a_1) + n(a_2))}} \right] && \text{since } \sqrt{x} + \sqrt{y} \leq \sqrt{2(x+y)} \\ &\geq \sqrt{\log n(p)} \left[\frac{1}{\frac{n(p)}{2} \sqrt{2 \cdot n(p)}} \right] && \text{since } n(a_1) + n(a_2) \leq n(p) \\ &= \sqrt{\frac{2 \log n(p)}{n(p)^3}} \\ &\geq \sqrt{\frac{2 \log N}{N^3}} \end{aligned}$$

Combining this bound with equation (9), we conclude that:

$$\frac{\bar{Q}(a_2) - \bar{Q}(a_1)}{\sqrt{\log n(p)} \left(\sqrt{\frac{1}{n(a_1)}} - \sqrt{\frac{1}{n(a_2)}} \right)} \leq \sqrt{\frac{N^3}{2 \log N}}$$

Thus, choosing a value for the exploration constant c that is larger than this quantity, as per equation (8), will force UCT to build a search tree in a breadth-first fashion.

We now conclude by arguing why such a node expansion strategy will lead to lookahead pathology. Without loss of generality, consider a game tree rooted at a minimizing choice node p (i.e., a minimizing node with minimax value -1). Let s^* denote an optimal child of p and let s denote a sub-optimal child. This means that s^* is a maximizing forced node and s is a maximizing choice node. The density of winning nodes from the maximizing perspective at depth $2d$ from s is then given by equation (1). Since s^* is a forced node, we cannot directly use equations (1) or (2). However, we observe that all the children of s^* are minimizing choice nodes, and thus, the density of winning moves from the minimizing perspective at depth $2d$ from s^* is given by f_{2d-1} . We can use the negamax transformation to recast this as the density of winning nodes from the maximizing perspective at depth $2d$ from s^* : this is given by $1 - f_{2d-1}$. For large values of d , we know from equations (6) and (7) that $f_{2d} + f_{2d-1} = 1$, or $f_{2d} = 1 - f_{2d-1}$. In other words, the density of $+1$ leaf nodes at depth $2d$ in the subtrees rooted at s^* and s approach the same value, for sufficiently large d . Since the average of the utilities of these leaves at level $2d$ will dominate the average of *all* the leaves in the respective subtrees, we conclude that in large enough search trees, UCT's estimate of $\bar{Q}(s^*)$ will approach its estimate of $\bar{Q}(s)$. In other words, the algorithm will not be able to tell apart optimal and sub-optimal moves as it builds deeper trees, even though we have access to the true minimax value of each node in this setting, leading to the emergence of pathological behavior. \square

D Game Engine Settings

We collected our Chess data using the Stockfish 13 engine, with the following configuration:

```
"Debug Log File": "",
"Contempt": "24",
"Threads": "1",
"Hash": "16",
"Clear Hash Ponder": "false",
"MultiPV": "1",
"Skill Level": "20",
"Move Overhead": "10",
"Slow Mover": "100",
"nodestime": "0",
"UCI_Chess960": "false",
"UCI_AnalyseMode": "false",
"UCI_LimitStrength": "false",
"UCI_Elo": "1350",
"UCI_ShowWDL": "false",
"SyzygyPath": "",
"SyzygyProbeDepth": "1",
"Syzygy50MoveRule": "true",
"SyzygyProbeLimit": "7",
"Use NNUE": "false",
"EvalFile": "nn-62ef826d1a6d.nnue"
```

We collected our Othello data using the Edax 4.4 engine¹ with the default settings. Edax is freely available online under a GNU GPL v3.0 license.

¹<https://github.com/abulmo/edax-reversi>

E Critical Rates in Othello

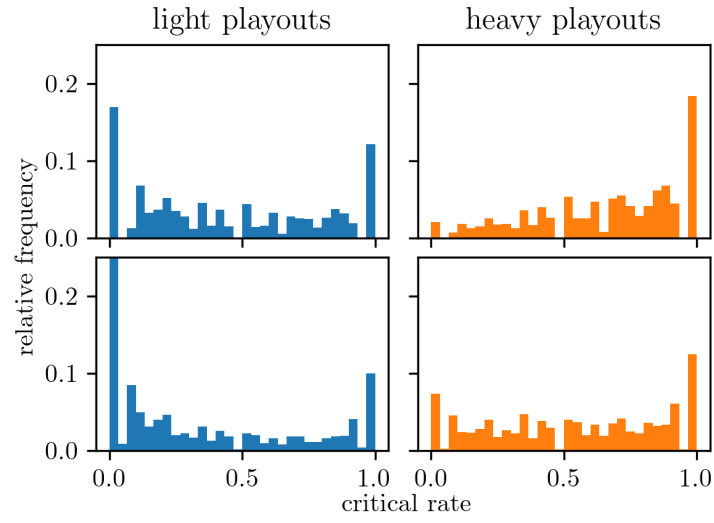


Figure 6: Histograms of empirical critical rates $(\tilde{\gamma})$ for Othello positions sampled $p = 10$ (top row) and $p = 36$ (bottom row) plies deep into the game. We sample the positions using both light playouts (left column) and heavy playouts (right column).

F Impact of Maximum Tree Depth on Pathology

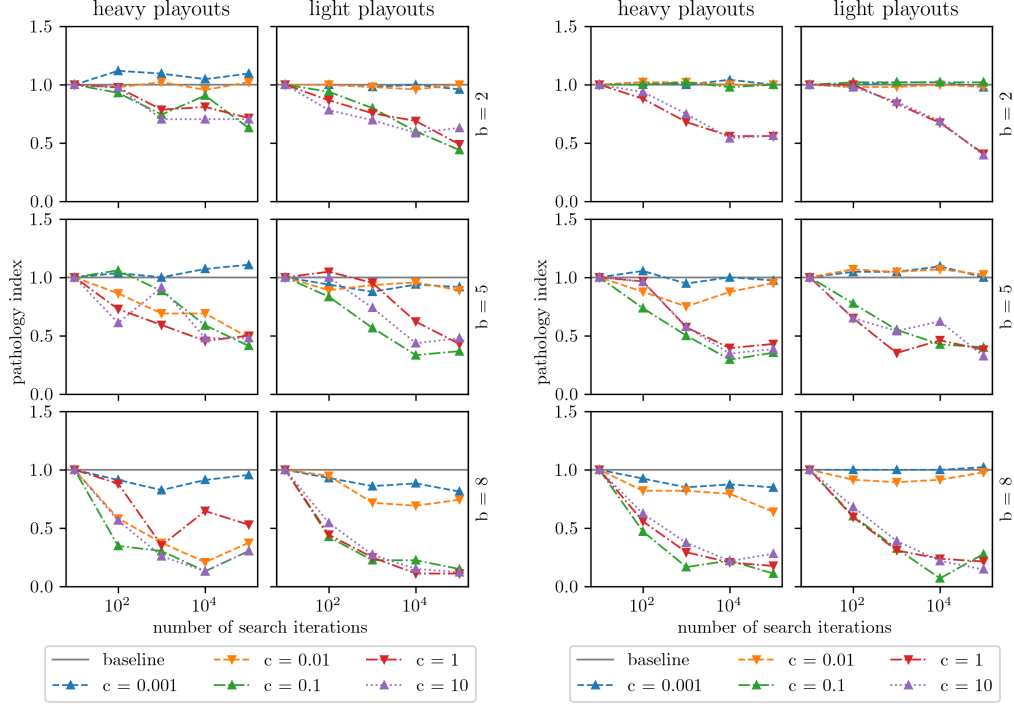


Figure 7: Measuring pathological behavior in UCT on critical win-loss games of depth 200 with $\gamma = 1.0$. The pair of plots on the left correspond to using a heuristic constructed from histograms of Stockfish evaluations of Chess positions sampled at depth 10, using both light and heavy playouts. The pair of plots on the right correspond to using a heuristic constructed from histograms of Edax evaluations of Othello positions sampled at depth 10, using both light and heavy playouts. Each colored line corresponds to an instantiation of UCT with a different exploration constant. The x -axis is plotted on a log-scale. We note the continued persistence of lookahead pathology.

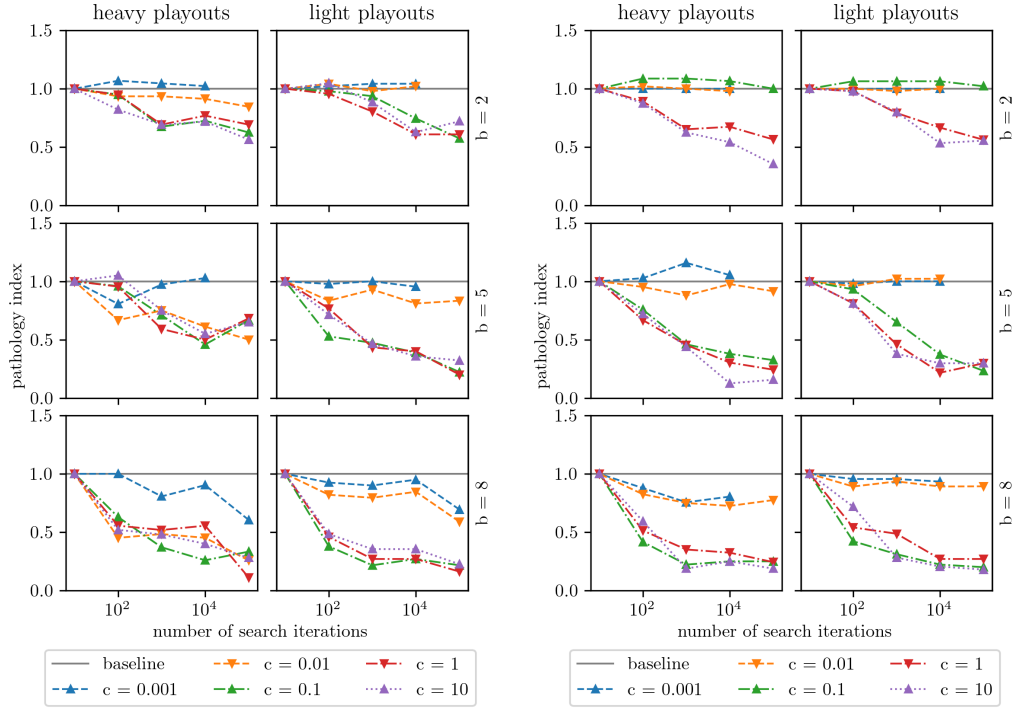


Figure 8: Measuring pathological behavior in UCT on critical win-loss games of depth 2000 with $\gamma = 1.0$. The pair of plots on the left correspond to using a heuristic constructed from histograms of Stockfish evaluations of Chess positions sampled at depth 10, using both light and heavy playouts. The pair of plots on the right correspond to using a heuristic constructed from histograms of Edax evaluations of Othello positions sampled at depth 10, using both light and heavy playouts. Each colored line corresponds to an instantiation of UCT with a different exploration constant. The x -axis is plotted on a log-scale. We note the continued persistence of lookahead pathology.

G Impact of Low Critical Rate on Pathology

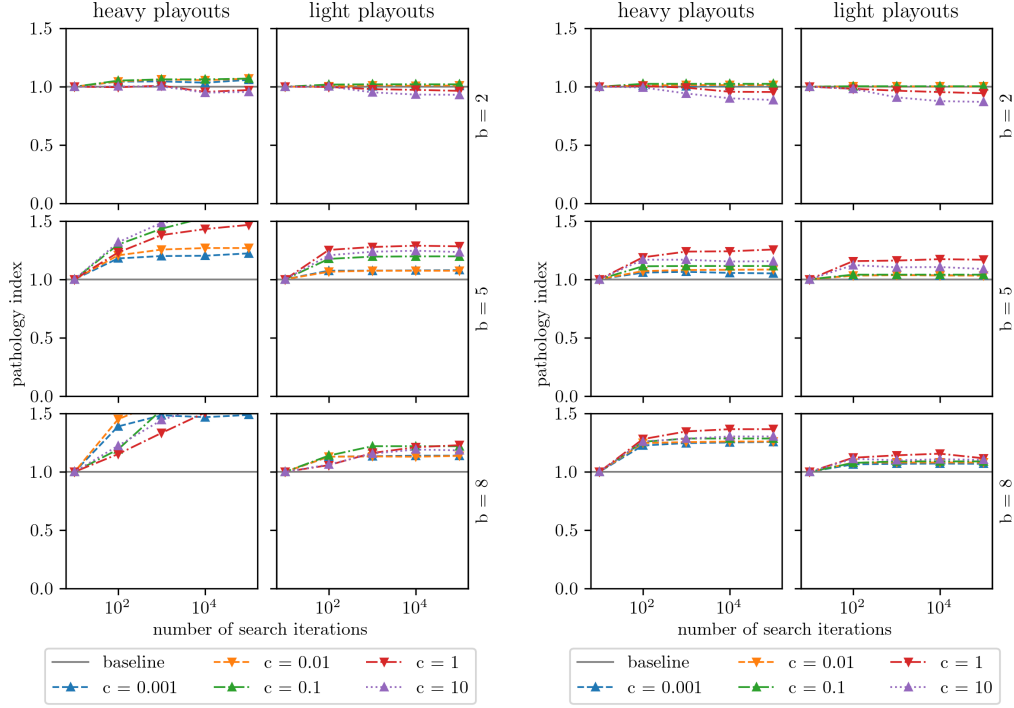


Figure 9: Measuring pathological behavior in UCT on critical win-loss games of depth 50 with $\gamma = 0.5$. The pair of plots on the left correspond to using a heuristic constructed from histograms of Stockfish evaluations of Chess positions sampled at depth 10, using both light and heavy playouts. The pair of plots on the right correspond to using a heuristic constructed from histograms of Edax evaluations of Othello positions sampled at depth 10, using both light and heavy playouts. Each colored line corresponds to an instantiation of UCT with a different exploration constant. The x -axis is plotted on a log-scale. We note the near complete absence of lookahead pathology in this low γ regime.

H Investigating Pathology with Othello-Derived Heuristics

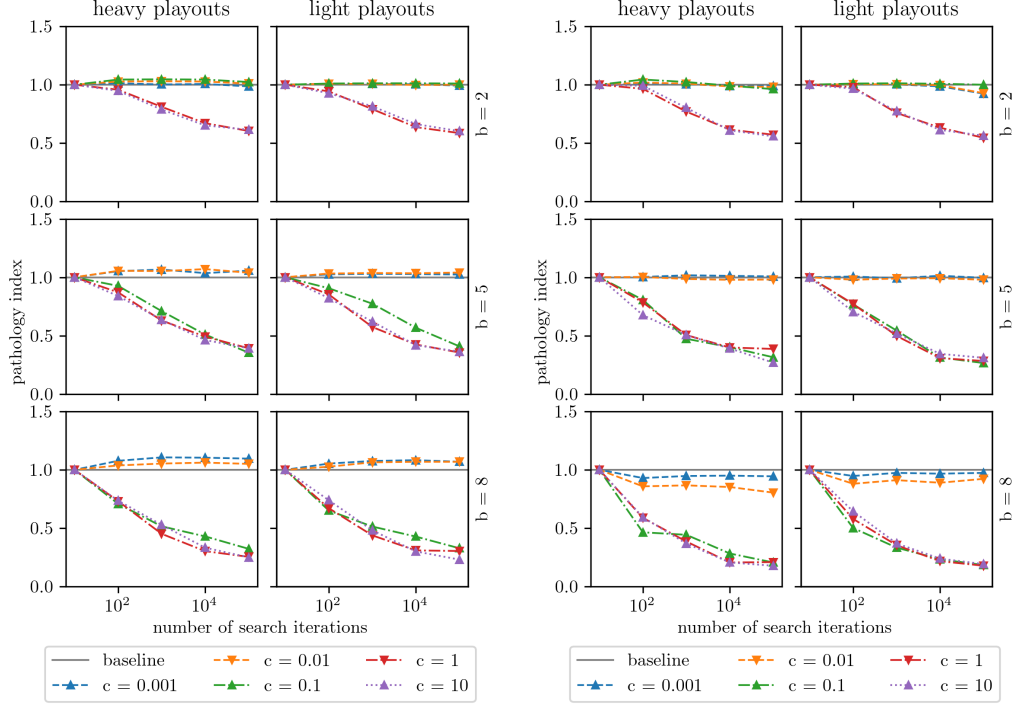


Figure 10: Measuring pathological behavior in UCT on critical win-loss games of depth 50 with $\gamma = 0.9$ (left) and $\gamma = 1$ (right). The heuristic to guide UCT is constructed from histograms of Edax evaluations of Othello positions sampled at depth 10, using both light and heavy playouts. Each colored line corresponds to an instantiation of UCT with a different exploration constant. The x -axis is plotted on a log-scale. We note that aside from some minor exceptions, pathological behavior generally persists even when the heuristic is sourced from a different domain.

I Investigating Pathology in Alpha-Beta Search

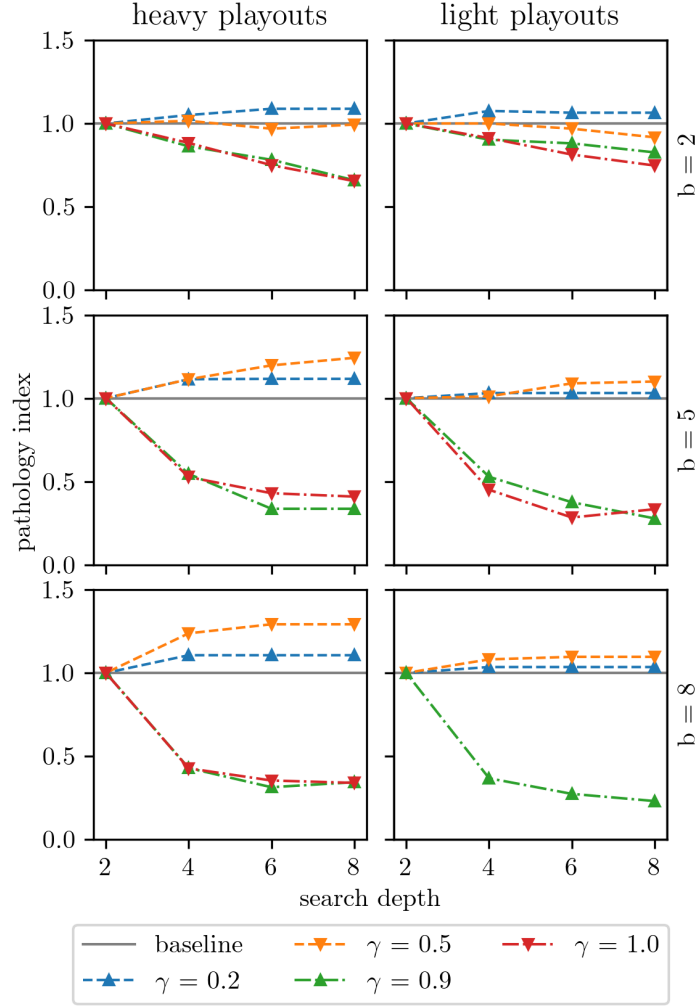


Figure 11: Measuring pathological behavior in alpha-beta search on critical win-loss games. The heuristic to guide the search constructed from histograms of Stockfish evaluations of Chess positions sampled at depth 10, using both light and heavy playouts. The x -axis indicates the depth of the search tree. Each colored line corresponds to a different choice of γ . We note that pathology occurs in a wide range of parameterizations, including smaller branching factors and moderate settings of γ , but is most pronounced for large values of γ .